

NASA/TP—2006-214232



# Two-Dimensional Simulation of Left-Handed Metamaterial Flat Lens Using Remcon XFDTD

*Jason M. Reinert*  
*Ohio Aerospace Institute, Brook Park, Ohio*

*Jeffrey D. Wilson*  
*Glenn Research Center, Cleveland, Ohio*

## NASA STI Program . . . in Profile

Since its founding, NASA has been dedicated to the advancement of aeronautics and space science. The NASA Scientific and Technical Information (STI) program plays a key part in helping NASA maintain this important role.

The NASA STI Program operates under the auspices of the Agency Chief Information Officer. It collects, organizes, provides for archiving, and disseminates NASA's STI. The NASA STI program provides access to the NASA Aeronautics and Space Database and its public interface, the NASA Technical Reports Server, thus providing one of the largest collections of aeronautical and space science STI in the world. Results are published in both non-NASA channels and by NASA in the NASA STI Report Series, which includes the following report types:

- **TECHNICAL PUBLICATION.** Reports of completed research or a major significant phase of research that present the results of NASA programs and include extensive data or theoretical analysis. Includes compilations of significant scientific and technical data and information deemed to be of continuing reference value. NASA counterpart of peer-reviewed formal professional papers but has less stringent limitations on manuscript length and extent of graphic presentations.
- **TECHNICAL MEMORANDUM.** Scientific and technical findings that are preliminary or of specialized interest, e.g., quick release reports, working papers, and bibliographies that contain minimal annotation. Does not contain extensive analysis.
- **CONTRACTOR REPORT.** Scientific and technical findings by NASA-sponsored contractors and grantees.

- **CONFERENCE PUBLICATION.** Collected papers from scientific and technical conferences, symposia, seminars, or other meetings sponsored or cosponsored by NASA.
- **SPECIAL PUBLICATION.** Scientific, technical, or historical information from NASA programs, projects, and missions, often concerned with subjects having substantial public interest.
- **TECHNICAL TRANSLATION.** English-language translations of foreign scientific and technical material pertinent to NASA's mission.

Specialized services also include creating custom thesauri, building customized databases, organizing and publishing research results.

For more information about the NASA STI program, see the following:

- Access the NASA STI program home page at <http://www.sti.nasa.gov>
- E-mail your question via the Internet to [help@sti.nasa.gov](mailto:help@sti.nasa.gov)
- Fax your question to the NASA STI Help Desk at 301-621-0134
- Telephone the NASA STI Help Desk at 301-621-0390
- Write to:  
NASA STI Help Desk  
NASA Center for AeroSpace Information  
7121 Standard Drive  
Hanover, MD 21076-1320



# Two-Dimensional Simulation of Left-Handed Metamaterial Flat Lens Using Remcon XFDTD

*Jason M. Reinert*  
*Ohio Aerospace Institute, Brook Park, Ohio*

*Jeffrey D. Wilson*  
*Glenn Research Center, Cleveland, Ohio*

National Aeronautics and  
Space Administration

Glenn Research Center  
Cleveland, Ohio 44135

## Acknowledgments

This work was supported by the NASA Glenn Research Center's Independent Research and Development Fund.

Trade names and trademarks are used in this report for identification only. Their usage does not constitute an official endorsement, either expressed or implied, by the National Aeronautics and Space Administration.

*Level of Review:* This material has been technically reviewed by an expert single reviewer.

Available from

NASA Center for Aerospace Information  
7121 Standard Drive  
Hanover, MD 21076-1320

National Technical Information Service  
5285 Port Royal Road  
Springfield, VA 22161

Available electronically at <http://gltrs.grc.nasa.gov>

# Two-Dimensional Simulation of Left-Handed Metamaterial Flat Lens Using Remcom XFDTD

Jason M. Reinert  
Ohio Aerospace Institute  
Brook Park, Ohio 44135

Jeffrey D. Wilson  
National Aeronautics and Space Administration  
Glenn Research Center  
Cleveland, Ohio 44135

## Summary

Remcom's XFDTD software was used to model the properties of a two-dimensional left-handed metamaterial (LHM) flat lens. The focusing capability and attenuation of the material were examined. The results showed strong agreement with both experimental results and theoretical predictions of focusing effects and focal length. Moreover, the inherent attenuation in the model corresponds well with the experimental results and implies that the code does a reasonably accurate job of modeling the actual metamaterial.

## Introduction

Recently there has been considerable interest in left-handed metamaterials (LHM), which are also known as double negative metamaterials or negative index materials. These materials are engineered so that their effective electrical permittivity  $\epsilon$  and magnetic permeability  $\mu$  values are negative over a specific frequency range. In 1968, Veselago (ref. 1) postulated that a flat piece of material with simultaneous negative values of  $\epsilon$  and  $\mu$  would alter the phase and group velocities of electromagnetic radiation so that they would propagate in opposite directions and also invert Snell's law of refraction, the Doppler effect, and Cherenkov radiation. Pendry et al. (refs. 2 and 3) first showed that a three-dimensional array of intersecting thin wires could be used to create negative values of  $\epsilon$  and that a periodic array of copper split-ring resonators could produce an effective negative  $\mu$ . In 2000 Smith et al. were the first to successfully combine the two arrays and produce a LHM which had negative values of  $\epsilon$  and  $\mu$  for a band of frequencies in the GHz range (ref. 4).

Wilson and Schwartz experimentally tested a flat lens constructed of LHM (ref. 5). They created a 20- by 20- by 3-unit cell array comprising copper split-ring

resonators and thin copper wires etched onto a fiberglass substrate. The entire block measured 100 by 100 by 10 mm, and a partial view is shown in figure 1. The LHM block was placed in a parallel-plate waveguide as shown in the photograph of its experimental setup (fig. 2). On one side of the LHM, a coaxial cable was attached to the top plate of the waveguide and the center conductor of the cable was fed through to the bottom plate. Cylindrical waves with a vertically directed electric field radiated from this source point and passed through the LHM. In order to detect the microwave power distribution after the waves had passed through the LHM, a detecting probe was attached to a computer-controlled x-y positioning stage and was scanned over a distance of 100 mm in the x-direction (toward and away from the LHM) and over a distance of 60 mm in the y-direction (from edge to edge in the waveguide). A top view of the experimental setup is shown schematically in figure 3. The LHM was placed at nine locations away from the source so that the front focal length (designated as ffl in fig. 3) ranged from 30 to 70 mm. The signal was swept from 9.50 to 12.50 GHz in 0.10-GHz intervals at each location. The back focal length (bfl), which for this experiment is defined as the distance from the back edge of the block to the power maximum along the x-axis (see fig. 3), was measured for each frequency. The results of the experiment at 10.30 GHz are shown in figure 4. A focusing effect can be seen around the  $y = 0$  axis. In addition, we find that the bfl decreases as the distance from the source increases.

Modeling the geometry of the split-ring resonators and wires of the left-handed metamaterial flat lens would be too memory intensive to simulate, so the Drude model for explaining conductivity in materials (refs. 6 and 7) was used to create homogeneous frequency-dependent materials with negative values of both  $\epsilon$  and  $\mu$ . In this report, the effectiveness of XFDTD in simulating LHMs will be examined along with the properties of a variable

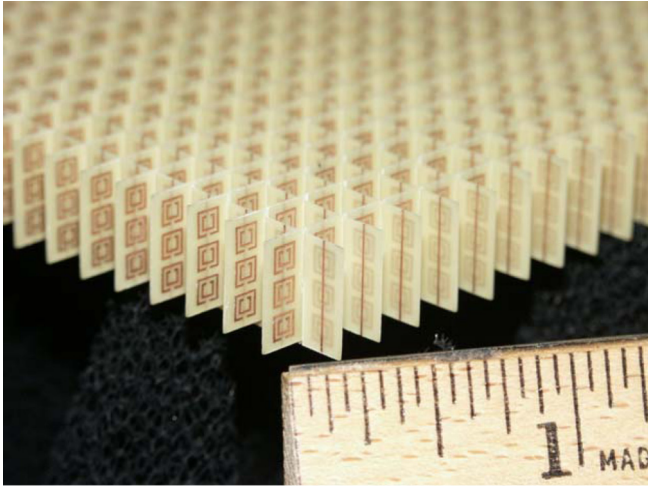


Figure 1.—Partial view of LHM block used by Wilson and Schwartz (ref. 5).

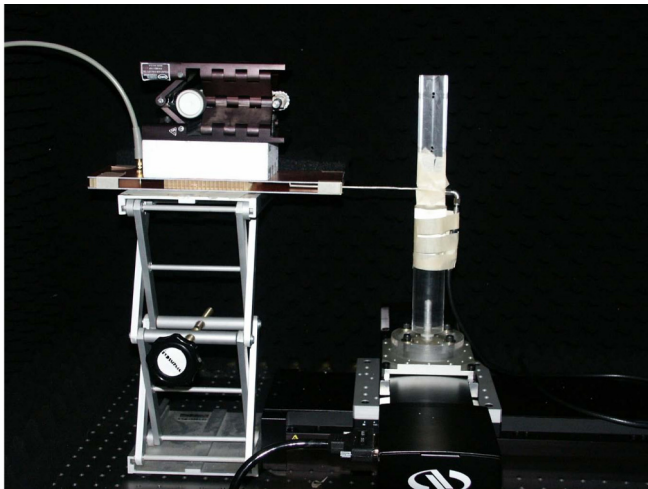


Figure 2.—Experimental setup of Wilson and Schwartz (ref. 5). On left side of LHM block, a coaxial cable is attached to top plate of waveguide and the center conductor of cable is fed through to bottom plate. Cylindrical waves with vertically directed electric field radiate from this source point and pass through LHM. To detect microwave power distribution after waves had passed through LHM, a probe is attached to computer-controlled x-y positioning stage and scans over 100 mm in x-direction (toward and away from LHM) and over 60 mm (from edge to edge in waveguide).

focal length flat lens constructed from these materials. The results will be compared to both earlier theoretical predictions (ref. 1) and Wilson and Schwartz’s experimental findings (ref. 5).

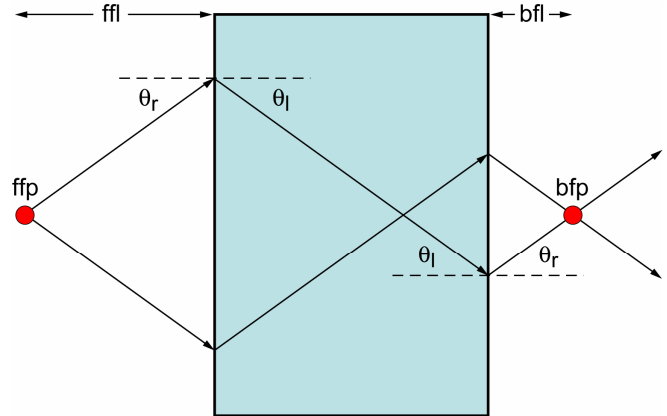


Figure 3.—Top view of experimental setup of Wilson and Schwartz (ref. 5). Source point is designated as front focal point (ffp); distance from this point to LHM block is front focal length (ffl). Shown is a ray entering LHM block at angle of refraction  $\theta_r$ . As it passes into LHM, the ray experiences negative refraction, with its angle changing from  $\theta_r$  to  $\theta_l$ . As it passes out of LHM it again experiences negative refraction, with its angle changing from  $\theta_l$  to  $\theta_r$ . This enables the radiation to focus at back focal point (bfp), with distance from LHM designated as back focal length (bfl).

## Modeling Left-Handed Metamaterial Flat Lens with Remcom XFDTD

Remcom XFDTD is a full wave three-dimensional electromagnetic solver. The terminology “full wave” indicates that no approximations are used in the calculation of electromagnetic waves. It utilizes the finite difference time domain method for solving Maxwell’s equations. This method allows the user to view the electric and magnetic fields in the time domain and the fields’ propagation over a period of time. The basic unit of calculation for this method is the Yee cell (ref. 7). This cell is a three-dimensional rectangular box that places electric field values on the edges of the cell and magnetic field values on the sides of the cell. This placement of the fields allows the program to quickly calculate field values by using shared sides and edges from other cells.

### Defining the Structure Geometry

For the first step, we need to define the geometry of the structure to be modeled. A screenshot of the XFDTD geometry screen is shown in figure 5. The largest portion of the screen is taken up by the geometry window. This

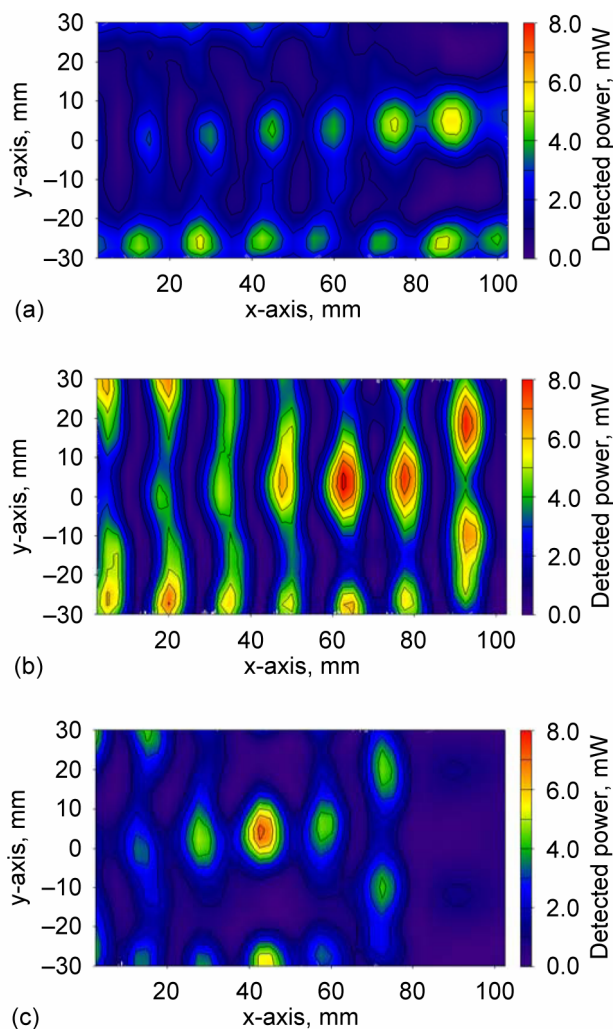


Figure 4.—Results from Wilson and Schwartz experiment at 10.30 GHz (ref. 5). (a) Front focal length (ffl) is 30 mm and corresponding back focal length (bfl) is 87.5 mm. (b) ffl is 50 mm and bfl is 60 mm. (c) ffl is 70 mm and bfl is 40 mm.

is where the actual drawing is shown. Three different planes—xy, yz, and zx—are shown in small screens to the left as well as the three-dimensional view. The large geometry can be oriented to any of these views by simply clicking on the smaller window. The object tree shows each element of the geometry that has been created. Clicking on an element will highlight it in the geometry window. The shape tabs allow the user to create a variety of three-dimensional volumes by specifying properties such as width or depth as well as assigning predefined material properties. A two-dimensional editor can be used for creating complex planar objects and can be opened in one of three ways: (1) pressing the 2D Editor icon on the geometry window toolbar while in solid mode, (2) right-clicking in the

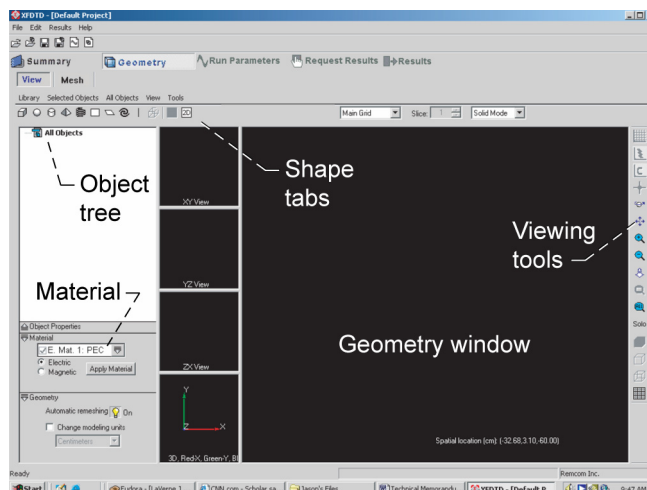


Figure 5.—Screenshot of XFDTD main geometry tab, where model and its materials are defined.

main view and choosing “2D Editor,” or (3) selecting “2D Editor” under [Tools] from the geometry window menu bar. This editor uses predefined shapes such as rectangles and ellipses, but also allows the user to draw a shape freehand. The drop-down menus above the buttons contain several features that are used to manipulate individual elements, although most of these features are also available by right-clicking on a specific part in the object tree. The material area is where the user is able to create a new type of material by defining certain parameters. Three default materials are defined: free space, perfect electric conductor (PEC), and perfect magnetic conductor (PMC); all other materials must be user defined. In XFDTD, a single material cannot be assigned both electric and magnetic properties. Thus to create a volume with both types of properties, both an electric and a magnetic material are assigned to occupy the same space in the geometry. Finally, the viewing tools allow the user to alter the view of the geometry by rotating the axes, panning, and zooming.

It is recommended to first define the materials before creating the structure. This way materials can be easily applied to objects as they are created. In the “Material” area, first select either “Electric” or “Magnetic” material. Both options offer the user several choices to customize a material. The user can define a name for a material along with material parameters and its viewing color.

Next the user must construct the structure of the geometry. This is done by using the shape tabs. XFDTD allows the user to create simple three-dimensional shapes such as rectangular boxes, spheres, pyramids and wires. Each object has a set of coordinates that must be defined before they are created. For example, a

rectangular box has two corner points that define its length, width, and depth. More complex three-dimensional shapes are created using Boolean expressions such as addition, subtraction, or intersection. A two-dimensional editor is available to create flat polygons or circles to be used in simulations. Unfortunately, no extrude option is available for these two-dimensional shapes. A computer-aided design (CAD) importer allows the user to bring in previously designed geometries to use with XFDTD and is recommended for more intricate geometries. XFDTD takes care of the meshing of the geometry once it has been imported.

## Mesh

We need to mesh the structure after defining its geometry. This involves breaking the structure into thousands of Yee cells. XFDTD has a default setting that balances memory usage with reasonable simulation time, which is good for most applications. It can also be set to mesh the structure into a user-defined number of cells, or the user can specify the dimensions of the cells to create more rectangular cell shapes. The user also has the option to define padding cells, or free space, surrounding the structure. The user can choose between a uniform amount of padding on each side or explicitly defining padding amounts on all six sides. XFDTD offers a color-coded view of each element and the padding surrounding it. Also, along the top of the view is the size of the mesh. It is necessary to consider this because the size will be a large factor in determining the run time of the simulation. The user must be aware of the amount of RAM the computer has because meshes that are too large will not run at all.

XFDTD comes with an adaptive mesh feature. Here, the user is able to specify certain regions of the mesh to refine. It is possible to define either exact cell dimensions or the ratio to the main mesh cell size in the specified direction. For example, if the main cell size is 1 mm, a specified ratio of 4:1 in the z-direction will provide a z-dimension length of 0.25 mm for the cells in the refined region. XFDTD automatically adjusts the cells sizes at the boundaries of the adaptive regions to transition back to the main cell size.

After the mesh is created the user can alter the mesh by using the [Mesh] edit tool. This allows the user to assign a different material to specific cells. The mesh edit feature is useful if a small change is needed, but large changes should be made by creating a new object.

## Material Characterization

The Drude model for explaining conductivity in materials, first proposed by Paul Drude in 1900 (refs. 6 and 7), was used to create the negative values of  $\epsilon$  and  $\mu$  in XFDTD. This model describes the interactions electrons have amongst each other and with other atoms (ref. 8). The materials used were created using this model in XFDTD, and the equations for it are

$$\epsilon_r(\omega) = \epsilon_\infty + \frac{(\epsilon_s - \epsilon_\infty)}{1 + j\omega t_0} + \frac{\sigma}{j\omega t_0} \quad (1)$$

$$\mu_r(\omega) = \mu_\infty + \frac{(\mu_s - \mu_\infty)}{1 + j\omega t_0} + \frac{\sigma_m}{j\omega t_0} \quad (2)$$

with  $\epsilon_\infty$  and  $\mu_\infty$  being the infinite frequency relative permittivity and permeability, respectively;  $\epsilon_s$  and  $\mu_s$  being the static relative permittivity and permeability, respectively;  $\sigma$  and  $\sigma_m$  being the electrical and magnetic conductivity, respectively;  $\omega$  being the angular frequency; and  $t_0$  being the relaxation time. To calculate the refractive index, first rewrite the equations into their real and imaginary parts:

$$\epsilon_r(\omega) = \epsilon' - j\epsilon'' \quad (3)$$

$$\mu_r(\omega) = \mu' - j\mu'' \quad (4)$$

such that

$$\epsilon' = \epsilon_\infty + \frac{(\epsilon_s - \epsilon_\infty)}{1 + (\omega t_0)^2} \quad (5)$$

$$\epsilon'' = \frac{(\epsilon_s - \epsilon_\infty)}{1 + (\omega t_0)^2} + \frac{\sigma}{\omega \epsilon_0} \quad (6)$$

The same form can be applied to the magnetic case. The refractive index  $n$  is defined by equation (7):

$$n(\omega) = \pm \sqrt{\epsilon(\omega)\mu(\omega)} \quad (7)$$

Electromagnetic waves will not propagate through a material whose refractive index is imaginary. Therefore, the signs of  $\epsilon(\omega)$  and  $\mu(\omega)$  must be the same. A negative sign for the square root must be chosen when both  $\epsilon$  and  $\mu$  are negative (ref. 9). By substituting equations (3) and



(4) into equation (7), the refractive index is

$$n = \pm \sqrt{(\epsilon' - j\epsilon'')(\mu' - j\mu'')} \quad (8)$$

After solving for the real part of  $n$  in equation (8), the following equation is obtained

$$n' = \pm \frac{\sqrt{2}}{2} \sqrt{(\epsilon' \mu' - \epsilon'' \mu'') + \sqrt{(\epsilon'^2 + \epsilon''^2)(\mu'^2 + \mu''^2)}} \quad (9)$$

where  $n'$  is the real part of the index of refraction. It can be seen that with proper selection of values, the real portions of the permittivity and permeability can become negative. These numbers cannot be selected randomly in order to achieve negative values because of software calculation limitations. These limitations are that the time step of the simulation must be smaller than 3 percent of the relaxation time,  $\epsilon_\infty$  and  $\mu_\infty$  should not be much larger than 1, and finally, if  $\epsilon_s < \epsilon_\infty$  and  $\mu_s < \mu_\infty$ —which is necessary to achieve negative  $\epsilon(\omega)$  and  $\mu(\omega)$ —then

$$\sigma \geq \frac{\epsilon_0(\epsilon_s - \epsilon_\infty)}{t_0} \quad (10)$$

and

$$\sigma_m \geq \frac{\mu_0(\mu_s - \mu_\infty)}{t_0} \quad (11)$$

To calculate acceptable values, this information was entered into a spreadsheet, and the values were altered until all conditions were met. The resulting values were  $\epsilon_\infty = 1.001$ ,  $\mu_\infty = 1.001$ ,  $\epsilon_s = -4269$ ,  $\mu_s = -4269$ ,  $\sigma = 54.02$ ,  $\sigma_m = 7.667 \times 10^6$ , and  $t_0 = 7.0 \times 10^{-10}$ . Using these values, a graph was created to show how the values of  $n'$  vary over a very narrow band of frequencies. This is shown in figure 6.

## Signals and Ports

A port is any side of a Yee cell in the mesh where a signal will be applied or a measurement will be taken. These ports can be added in two ways. The first is by simply going under the [Run Parameters → Component Ports] tab and entering in the cell location, orientation, polarity, and component type. A second and easier way

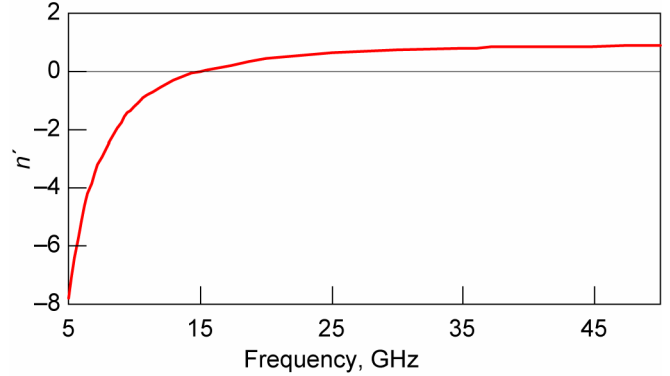


Figure 6.—Real part of index of refraction  $n'$  as function of frequency calculated with Drude model.

is to view the geometry in the [Mesh] mode and right-click on the desired cell. Next select “Edit Port” on the menu that appears. This takes the user to the [Component Ports] tab as well, but all of the cell information has already been entered.

After all port parameters have been set, the type of signal must be defined. This is done under the [Run Parameters → Source Type] tab. Here, the user can define a plane wave, discrete source, or a Gaussian beam and the polarity of the signal. Next, the shape of the signal is selected under the [Waveform] tab. The user can choose to examine a broadband result with a Gaussian pulse, Gaussian derivative, or modulated Gaussian or look at a steady-state result with a sinusoid. The user also has the option to create a unique type of signal by using the “User Defined” option. Finally, boundary conditions can be set under the [Outer Boundary] tab. A boundary can be a Perfect Electric Conductor (PEC), Perfect Magnetic Conductor (PMC), Liao, or Perfectly Matched Layer (PML). The PEC boundary is used when there is a conducting surface at the boundary. Both PEC and PMC boundaries can be used to take advantage of geometry symmetries to reduce the size of the mesh and the calculation time (ref. 10). The Liao boundary (ref. 11) is an absorbing boundary, which is usually quick and accurate, but it does produce instabilities in the calculations if objects are placed too close to the boundary. The PML boundary (ref. 12) is an absorbing boundary that is more robust than the Liao boundary, but the method of calculation is more complex and adds a significant amount of time to the simulation.

## Request Results

In the final step before the simulation can be run, the user must decide in which plane(s) to view the output

data. Once again, this can be done in two ways. Under the [Request Results] tab, the user selects the type of output to be calculated. Common types are near-zone fields and far-zone fields, but the transient field snapshots option is also very useful. This option saves a sequence of the electric field  $\mathbf{E}$ , magnetic field  $\mathbf{H}$ , current density  $\mathbf{J}$ , and Poynting vector  $\mathbf{S}$  values that can be viewed individually or as an animation in the [Geometry → View] tab after calculations.

### Postcalculation

After calculations have been run, there are a variety of results that can be examined. Already mentioned are the movies of the fields, but they are made even more useful by providing the feature to view them in vector format. This allows the user to view not only the magnitude of the field but also its orientation as it rotates through space. Also useful are the plots that XFDTD offers. The user has several options to view such as voltage versus time or impedance versus frequency. There are also options for far field calculations or fast Fourier transforms. S-parameter calculations are available for examining multiple port systems, but these must be turned on before calculations are run.

### Results

A block of electric material and a block of magnetic material were created so that both blocks occupied the same space. A sinusoidal source was added on the left side of the block with a frequency of 10.5 GHz. Only the transient fields were requested for these simulations. Figure 7 shows the results from simulations with the metamaterial blocks 30, 50, and 70 mm to the right of the source. The material is represented by the white outline, and the wave is traveling left to right. When the waves travel across the boundary of the material, the shape of the resultant waves appear to be the mirror image of the incident wave, and a focusing effect can be seen inside the material. The sharpness of the focal point, though, has been slightly degraded. In the animation of these waves, they actually appear to be traveling in opposite directions; the reason for this is the opposite directions of the group and phase velocities created by the negative values of  $\epsilon$  and  $\mu$  (ref. 1). After the wave comes to a focus, it once again reverts back to the shape of the original wave, although the strength of the wave has attenuated. When the wave encounters the second boundary, the shape is once again reversed and begins to focus. This focal point also produces a highly

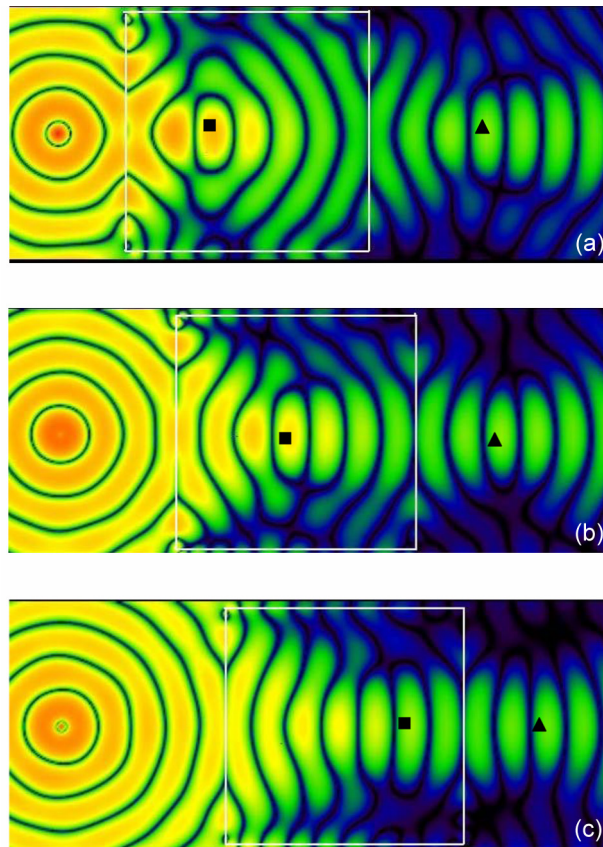


Figure 7.—Results of XDFTD simulations for LHM flat lens, with LHM block to right of source. A focal point, inside LHM block, is indicated by ■. Back focal point, on right side of LHM block, is indicated by ▲. Intensity of field is represented by color, with red being the strongest and blue the weakest. (a) LHM block is 30 mm from source and back focal length (bfl) is 58 mm. (b) LHM block is 50 mm from source and bfl is 40 mm. (c) LHM block is 70 mm from source and bfl is 27 mm.

attenuated wave, and it can clearly be seen that the resolution of the focal point has greatly deteriorated.

A flat lens made from a LHM should theoretically be able to change its focal length by adjusting the distance of the material from the source (ref. 5). This was tested by running three simulations with the LHM lens 30, 50, and 70 mm away from the source. The results for the three tests are shown in figure 7. These results correspond to the theoretical and experimental results obtained by Wilson and Schwartz (ref. 5) that were shown in figure 4. It can be seen that as the lens moves away from the source, the back focal length (bfl) becomes shorter. With the lens 30, 50, and 70 mm from the source, the bfls were approximated to be 58, 40, and 27 mm, respectively. It can also be noticed that the second focal point becomes less defined as the LHM

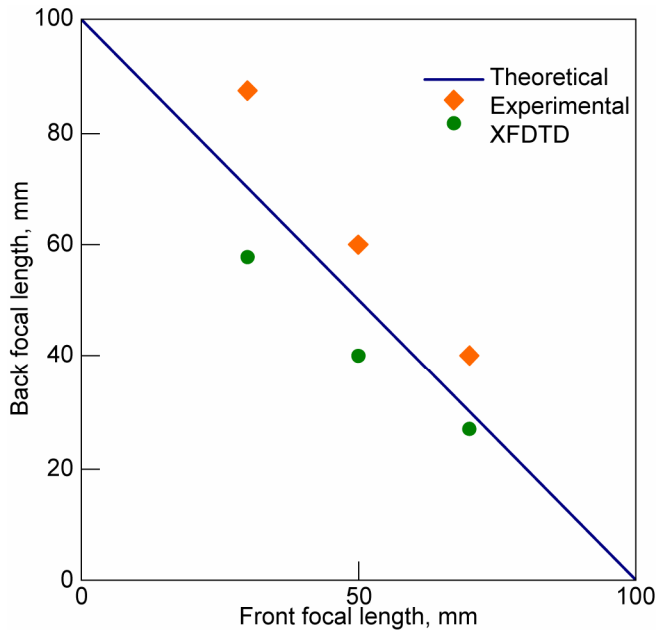


Figure 8.—LHM flat lens focal lengths modeled with XTDFD compared with theoretical and experimental results of Wilson and Schwartz (ref. 5).

block is moved further away from the source. Figure 8 shows these results along with Wilson and Schwartz's results. Both the XFDTD and experimental results agree moderately well with the theoretical values.

A large amount of attenuation, as much as 16.1 dB, was also noticed in the experimental results. A higher degree of attenuation of about 25 dB was noticed in the XFDTD simulations. The extent of the attenuation of the signal in XFDTD is determined by the parameters in the Drude equations. Less attenuation and better matching with experiment might be possible by using different values in the Drude equations with frequencies outside of the range considered.

## Conclusions

A variable focal length flat lens constructed from LHMs was simulated in XFDTD (Remcom). Drude equations can be used to simulate negative values of electrical permittivity and permeability if the parameters are set very carefully. XFDTD exhibited the ability to calculate the fields for LHMs and illustrated the effect of a wave having opposite values of phase velocity and group velocity. A flat lens made from this material did indeed show a focusing effect despite very high attenuation in all simulations. The focal length was varied by adjusting the distance of the lens from the source. At 30 mm from the source the back focal length

(bfl) was approximately 58 mm, at 50 mm from the source bfl was 40 mm, and at 70 mm from the source the bfl was 27 mm; these compared moderately well with theoretical values.

## References

1. Veselago, V.G.: *Electrodynamics of Substances With Simultaneously Negative Values of  $\epsilon$  and  $\mu$* . *Soviet Phys. Uspekhi*, vol. 10, no. 4, 1968, pp. 509–514.
2. Pendry, J.B., et al.: *Extremely Low Frequency Plasmons in Metallic Mesostructures*. *Phys. Rev. Lett.*, vol. 76, no. 25, 1996, pp. 4773–4776.
3. Pendry, J.B., et al.: *Magnetism From Conductors and Enhanced Nonlinear Phenomena*. *IEEE Trans. Microwave Theory Tech.*, vol. 47, no. 11, 1999, pp. 2075–2084.
4. Smith, D.R., et al.: *Composite Medium With Simultaneously Negative Permeability and Permittivity*. *Phys. Rev. Lett.*, vol. 84, 2000, pp. 4184–4187.
5. Wilson, Jeffrey D.; and Schwartz, Zachary D.: *Multifocal Flat Lens With Left-Handed Metamaterial*. *Appl. Phys. Lett.*, vol. 86, 2005, pp. 021113–1—021113–3.
6. Drude, P.: *Zur Electronentheorie I*. *Ann. Phys.*, vol. 1, 1900, pp. 566–613.
7. Drude, P.: *Zur Electronentheorie II*. *Ann. Phys.*, vol. 3, 1900, pp. 369–402.
8. Kunz, Karl S.; and Luebbers, Raymond: *The Finite Difference Time Domain Method for Electromagnetics*. CRC Press, Boca Raton, FL, 1993.
9. Smith, D.R.; and Kroll, N.: *Negative Refractive Index in Left-Handed Materials*. *Phys. Rev. Lett.*, vol. 85, no. 14, 2000.
10. Maruschek, J.W.; Kory, C.L.; and Wilson, J.D.: *Generalized Three-Dimensional Simulation of Ferruled Coupled-Cavity Traveling-Wave-Tube Dispersion and Impedance Characteristics*. NASA TP-3389, 1993.
11. Liao, Z.P., et al.: *A Transmitting Boundary for Transient Wave Analysis*. *Scientia Sinica A*, vol. 27, no. 10, 1984, pp. 1063–1076.
12. Berenger, J.P.: *A Perfectly Matched Layer for the Absorption of Electromagnetic Waves*. *J. Comput. Phys.*, vol. 114, no. 1, 1994, pp. 185–200.

# REPORT DOCUMENTATION PAGE

*Form Approved*  
*OMB No. 0704-0188*

Public reporting burden for this collection of information is estimated to average 1 hour per response, including the time for reviewing instructions, searching existing data sources, gathering and maintaining the data needed, and completing and reviewing the collection of information. Send comments regarding this burden estimate or any other aspect of this collection of information, including suggestions for reducing this burden, to Washington Headquarters Services, Directorate for Information Operations and Reports, 1215 Jefferson Davis Highway, Suite 1204, Arlington, VA 22202-4302, and to the Office of Management and Budget, Paperwork Reduction Project (0704-0188), Washington, DC 20503.

<b>1. AGENCY USE ONLY</b> ( <i>Leave blank</i> )	<b>2. REPORT DATE</b> August 2006	<b>3. REPORT TYPE AND DATES COVERED</b> Technical Paper	
<b>4. TITLE AND SUBTITLE</b> Two-Dimensional Simulation of Left-Handed Metamaterial Flat Lens Using Remcon XFDTD		<b>5. FUNDING NUMBERS</b>  WBS 423799.03.01	
<b>6. AUTHOR(S)</b>  Jason M. Reinert and Jeffrey D. Wilson			
<b>7. PERFORMING ORGANIZATION NAME(S) AND ADDRESS(ES)</b>  National Aeronautics and Space Administration John H. Glenn Research Center at Lewis Field Cleveland, Ohio 44135-3191		<b>8. PERFORMING ORGANIZATION REPORT NUMBER</b>  E-15479	
<b>9. SPONSORING/MONITORING AGENCY NAME(S) AND ADDRESS(ES)</b>  National Aeronautics and Space Administration Washington, DC 20546-0001		<b>10. SPONSORING/MONITORING AGENCY REPORT NUMBER</b>  NASA TP-2006-214232	
<b>11. SUPPLEMENTARY NOTES</b>  Jason M. Reinert, Ohio Aerospace Institute, 22800 Cedar Point Road, Brook Park, Ohio 44142; Jeffrey D. Wilson, Glenn Research Center. Responsible person, Jeffrey D. Wilson, organization code RCE, 216-433-3513.			
<b>12a. DISTRIBUTION/AVAILABILITY STATEMENT</b>  Unclassified - Unlimited Subject Category: 70  Available electronically at <a href="http://gltrs.grc.nasa.gov">http://gltrs.grc.nasa.gov</a>  This publication is available from the NASA Center for AeroSpace Information, 301-621-0390.		<b>12b. DISTRIBUTION CODE</b>	
<b>13. ABSTRACT</b> ( <i>Maximum 200 words</i> )  Remcom's XFDTD software was used to model the properties of a two-dimensional left-handed metamaterial (LHM) flat lens. The focusing capability and attenuation of the material were examined. The results showed strong agreement with experimental results and theoretical predictions of focusing effects and focal length. The inherent attenuation in the model corresponds well with the experimental results and implies that the code does a reasonably accurate job of modeling the actual metamaterial.			
<b>14. SUBJECT TERMS</b>  Metamaterial; Refraction; Microwaves; Lens		<b>15. NUMBER OF PAGES</b>  13	<b>16. PRICE CODE</b>
<b>17. SECURITY CLASSIFICATION OF REPORT</b>  Unclassified	<b>18. SECURITY CLASSIFICATION OF THIS PAGE</b>  Unclassified	<b>19. SECURITY CLASSIFICATION OF ABSTRACT</b>  Unclassified	<b>20. LIMITATION OF ABSTRACT</b>



